DC FURNACE CONTAINMENT VESSEL DESIGN USING COMPUTATIONAL FLUID DYNAMICS

B. Henning[1], M. Shapiro[2] and L.A. le Grange[3]

[1]B. Henning, DC Arc Furnace Division, Bateman Metals, South Africa. E-mail: bennie.henning@batemanbv.com
[2]M. Shapiro, DC Arc Furnace Division, Bateman Metals, South Africa. E-mail: mike.shapiro@batemanbv.com
[3]L.A. le Grange, CFD Software Developer, Flo++®, South Africa. E-mail: louis@softflo.com

ABSTRACT

Effective pyrometallurgical process vessel design requires accurate assessment of the heat fluxes through the walls of the furnace. This is particularly important for freeze lining operation which is designed to protect refractory materials exposed to chemically corrosive molten contents, or facilitate high temperature operation when the refractory materials are used at conditions close to their service limits.

Numerical modelling of fluid flow and heat transfer in process vessels is often used to aid in the design of process vessels. Sophisticated models are used to analyse the three dimensional flow and heat transfer predicting the effects of electrical heating, magnetic stirring, buoyancy, shear forces, various cooling effects and ultimately heat fluxes at the walls of the furnace and refractory. Traditionally these models are applied to the separate single fluid systems in a vessel such as the freeboard region including the arc, the slag region and the metal bath. Boundary conditions such as shear forces and heat fluxes between connecting regions such as the slag and metal bath are either estimated or carried over from separate solutions.

Shortcomings in these traditional approaches include the estimation of sometimes critical boundary conditions leading to unreliable heat flux calculations. Also when boundary conditions are carried over between solutions, the process is difficult to set up, time-consuming and finally not fully coupled.

In this paper the definition and results of a fully integrated numerical model of a complete arc furnace are presented. The most important mechanisms acting in an arc furnace were considered, including the fields of electrical potential, current, magnetism, momentum, heat transfer and radiation. Temperature dependant properties included electrical conductivity, density, viscosity, and thermal conductivity. The geometry consists of the freeboard, the arc, slag, metal baths and different refractory regions. Although the combined model of air, slag and metal would be defined as a multi-phase problem it is not solved as such. Instead the different fluids are separated by sets of special solid baffles. These baffles allow the implicit transfer of current, magnetism, heat transfer and shear forces between the different fluids and disallow mixing of the separate fluids.

The strengths of the integrated model are threefold: Firstly, it provides robustness in defining the geometry and boundary conditions for the overall model. Secondly, it provides the capability to switch on and off individual mechanisms such as buoyancy, magnetic stirring and shear forces in order to observe their individual importance. Finally, it provides a useful tool in the design process through its ability to obtain results of parameter changes in short time scales.

1. INTRODUCTION

High intensity pyrometallurgical smelting and melting processes employing DC plasma arcs as the energy input source have increased the demands on the performance of the containment vessel refractory lining. DC furnaces normally operate with open baths in which molten process liquids are in direct contact with the refractory lining. The high reaction kinetics associated with vigorously stirred baths reduces black top formation of un-reacted material floating on the slag surface, thereby increasing freeboard-operating temperatures by radiation and convection. This combined with processes involving chemically aggressive

slag and superheated phases have made understanding the influence of the arc on velocities and temperature gradients within the molten bath critical to successful vessel design.

The open arc offers significant additional operating flexibility, as the total effective furnace resistance can be adjusted by operating with different arc lengths, thereby ensuring maximum power input over a wide range of bath resistance. This change in distribution of total power between the arc and the bath results in a trade-off between excessive radiation loading in the freeboard and increasing forced convection in the bath. Bath convection has a direct influence on freeze lining thickness and mechanical stability, and it also affects the erosion of protective partially reacted raw material side wall banks. Higher bath convection film coefficient increases the refractory hot face temperature.

The goal of this research was to develop a parametric model in a suitable Computational Fluid Dynamics (CFD) package, which would enable both design and operating parameters to be assessed and optimised.

The development plan included:

- Applying fundamental boundary conditions of current, anode potential and external temperatures to limit the number of assumptions required for model generation.
- Inclusion of temperature dependant properties (if published).
- Analysis within a single model without the need to transfer partial results between sub-analysis steps.
- Conjugate heat transfer[1] to obviate the need for assumptions of convection heat transfer coefficients.
- Joule (resistance) heating estimated directly from current distribution, and local resistivity.
- Parametric mesh generation to enable the geometry and boundary condition to be conveniently varied without the need to start each model from fundamental input commands.
- Control of relaxation factors and other numerical methods to ensure stability during the solution, which would be applicable to a wide range of geometries and operating parameters.
- Post processing[2] to allow convenient interpretation and comparison of results.

Furnace design parameters include:

- Overall furnace geometry.
- Cooling systems.
- Refractory composite selection (based on thermal conductivity).

Furnace operating parameters include:

- Furnace inventory levels and tapping cycle management.
- Selection of furnace electrical operating parameters (volts and amps to achieve a certain input power, arc length proportional to operating voltage).

2. APPROACH METHODOLOGY

The solution of the velocity, pressure and temperature fields in an atmospheric DC Plasma Arc has been well published in the literature [1,2,3,5,6]. In addition to the solution of the turbulent transport equations, and conservation of mass, momentum, and energy, the Maxwell equations have to be solved for the Lorentz forces as an additional source term in the momentum conservation equations (refer to Appendix A for the brief description of the conservation and MHD equations) [3], [5]. Simplified Maxwell equations may be solved because the flow satisfies the assumption associated with the magneto hydrodynamic flow (MHD) approximation [3], [5].

Papers have also been published on models and solution techniques which have been developed to include the interaction of the arc with the molten bath, and combine various source terms of the overall flow to establish which dominates in a given process [4,6]. These generally involve sequential type analysis because the arc flow influences the forced convection of the fluid with which the moving freeboard gases are in contact. Buoyancy driven convection, magnetic stirring and other momentum sources in the bath does not significantly influence the arc.

[1] Simultaneous, coupled heat transfer within a fluid and an adjoining solid.
[2] Post-processing of numerical results, whether data or visual representation.

In order to achieve the goals of this research, and generalise the arc and bath models to include for multiple liquid zones, and conjugate heat transfer in the refractory material in contact with liquid zones, the development team of Flo++® was approached to incorporate the Lorentz Forces as well as cathode and anode phenomena, following the approach of Jonas Alexis [3], [5]. This substantially reduced the overall time to develop the arc-bath model, because the pre-processor, conjugate heat transfer and post processor modules were already completed and thoroughly tested. In order to handle multiple fluid regions, and additional governing equations at the anode and cathode, baffle cell groups were developed.

The baffle cell group is a surface element with the following properties:

- Separates and confines each region to avoid analysis of the free surface between the freeboard and the slag, which would otherwise require full transient analysis instead of the quasi-steady state approach adopted.
- Withstands a pressure differential across the baffle to prevent the separated fluids from mixing.
- Facilitates continuity of conduction mechanisms, including heat flux, magnetic and electrical fields.
- Ensures shear force equilibrium across the baffle by a numerical approximation in which the momentum equation for cells adjacent to the baffle is solved using a combined viscosity between the two fluids.
- Prescribes special boundary conditions including cathode current density distribution, carbon sublimation temperature, Thompson Effect, Electrode Condensation, Anode Potential [5].
- Post processing to enable heat fluxes between regions to be extracted.

The code makes provision for switching flow and heat transfer mechanisms in different regions off and on, as well as varying numerical damping factors at different times during solution. These features are controlled by user defined sub-routines which enable the model to be solved sequentially, as well as allowing the coupled fields in each zone to build up gradually and quasi-simultaneously. This pseudo-transient approach promotes numerical stability during the initial part of the solution. All zones are solved simultaneously and implicitly in pseudo-steady state when the fields in each zone are sufficiently established. The code and user defined sub-routines were tested for numerical stability and conservation of transport mechanisms.

3. NUMERICAL MODEL

Prototype model geometry was developed based on a typical DC Slag Cleaning Furnace rated at 40 MW. However the input power was limited to 5 MW, which corresponds to the heat loss for a furnace of this size. A process energy dissipation sink has not yet been incorporated. The model configuration and position of the baffle cell groups is shown in Fig. 1. The model represents a 5-degree slice of the furnace with cyclical boundary conditions on the vertical slicing surfaces to preserve the symmetry.

Other key model parameters were:

- Input current 20 kA (held constant whilst arc length was varied).
- Operating Power 5 MW to approximate heat loss conditions (no process energy supplied).
- Electrode External Diameter 600 mm.
- Hearth Internal Diameter 9m.

The model is divided into 4 main regions (as shown in figure 1):

- The arc and upper freeboard region. The maximum cell size in the arc region corresponds to the cathode spot radius, determined by the applied current[3]. A radiation model based on a temperature-energy density look-up table is included as a heat transfer mechanism in this area to transfer heat from the arc to the slag surface and the refractory walls with temperature-dependant physical properties [3], [5].
- Slag bath with constant physical properties typical of Silica-Iron Oxide Slag [6]. Depth of slag at the top of the metal bath = 0.55m, which is the typical inventory for a 40 MW furnace.
- Metal bath with constant physical properties typical of molten steel [6]. Depth of metal at the lowest point of the hearth = 0.52m, which is the typical inventory for a 40 MW furnace.
- Refractory lining with constant physical properties typical of a DC Furnace set-up.

[3] $R_C=\sqrt{(I/\pi J_C)}$

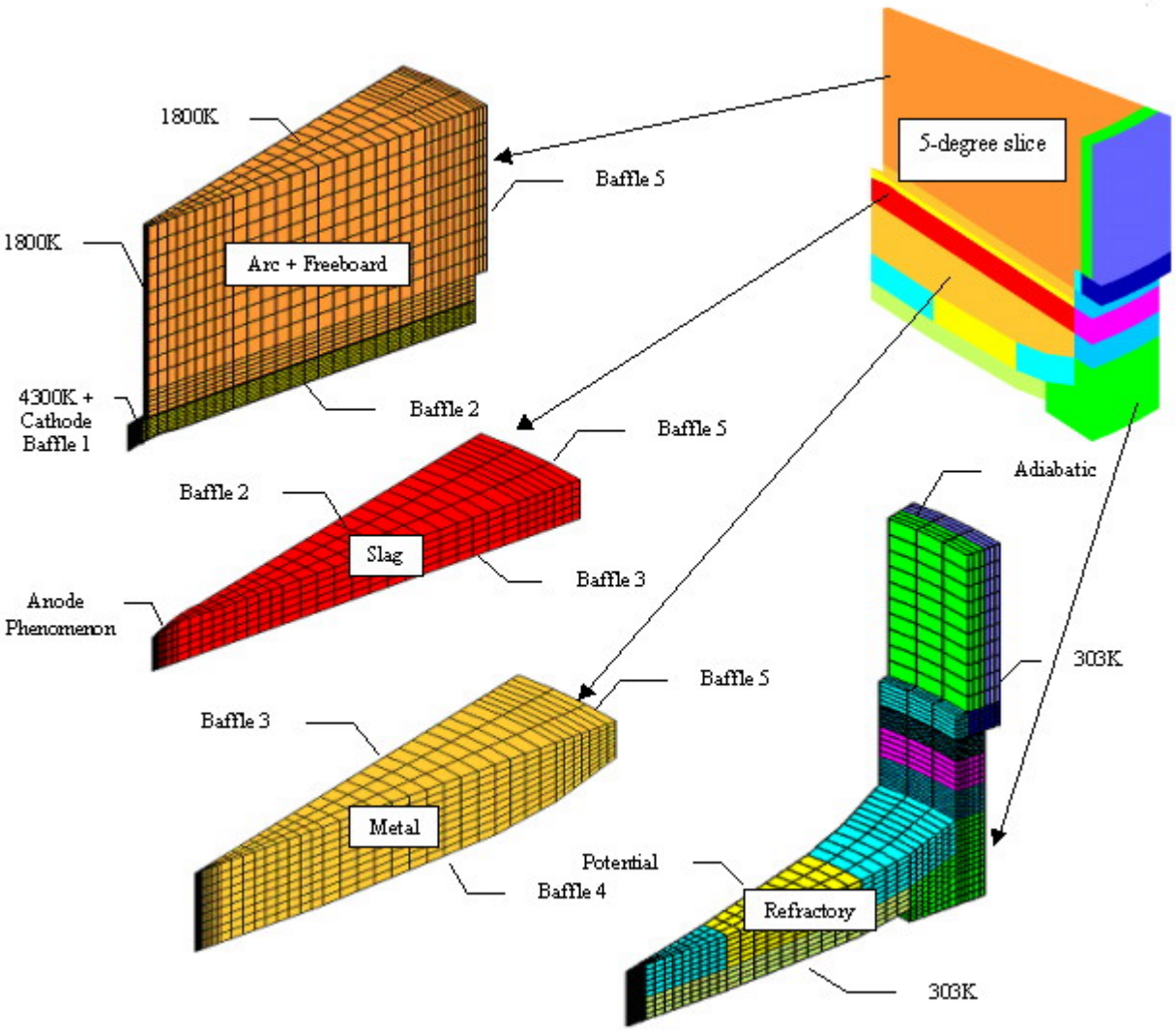

Figure 1. Composite layers of the numerical mesh for a typical DC Arc Furnace.

The model requires 5 main baffles to link the fluid and refractory regions:

- Tip of the electrode (cathode) and arc region interface. This area incorporates the necessary modelling of the cathode spot.
- Slag-freeboard interface. Selected areas include provision for modelling of anode phenomena. This area incorporates a predetermined, non-equilibrium arc depression zone to investigate the deflection of the hot gas in the arc away from the slag surface, and towards the upper side walls above the slag-freeboard interface.
- Slag- metal interface.
- Metal-hearth interface. This baffle incorporates the anode potential boundary condition.
- Molten slag, metal, arc and freeboard refractory interfaces.

Temperature and heat flux boundary conditions include:

- 4300 K fixed electrode tip temperature (carbon graphite sublimation temperature).
- 1800 K fixed electrode vertical surface temperature.
- 1800 K fixed inside furnace roof temperature (to simulate forced cooling of the roof).
- Adiabatic top of side wall surface.
- 303 K fixed cold face refractory temperature.

The following assumptions were made in the development of the numerical model:

- The arc geometry is axi-symmetric and time independent.
- The current distribution in the arc column is parabolic [5].
- Heat conduction and internal heat generation in the electrode was ignored
- The velocity, temperature, magnetic and other fields were allowed to develop over a number of time steps as if the various physical phenomena were gradually switched on over time.
- When the fields are changing slowly, (quasi-static), the model is converted to a time independent analysis.
- Logarithmic wall functions were incorporated in the wall boundary specification [7] instead of solving the detail boundary layers necessitating very fine grids.

4. DISCUSSION OF THE NUMERICAL RESULTS

For illustration purposes, the temperature and velocity fields in the arc and freeboard regions are shown at an arc length of *16 cm* in Figures 2 to 5. The velocity and temperature fields in the slag bath are shown in Figures 6 and 7 and the velocity and temperature fields in the metal bath are shown in Figures 8 and 9. All temperatures are in Kelvin and relative to zero Kelvin.

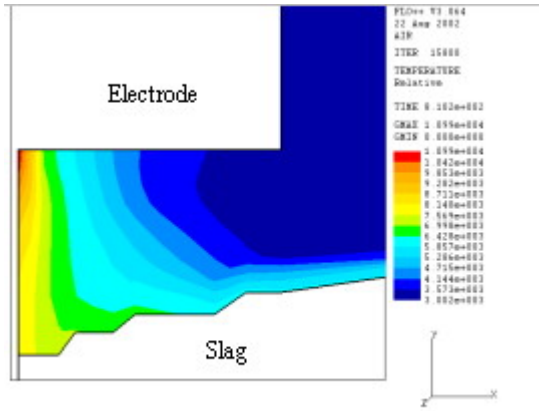

Figure 2. Temperature contour distribution in the arc region.

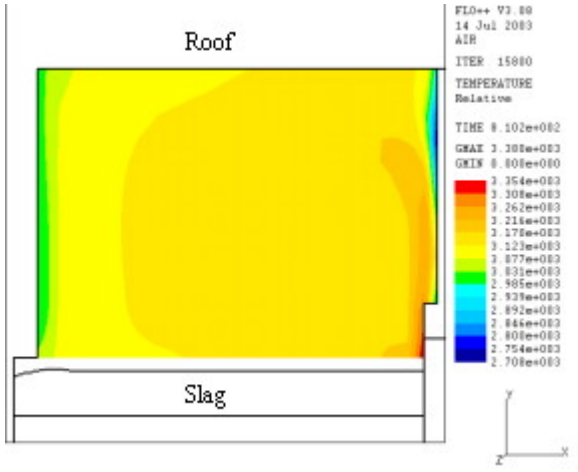

Figure 3. Temperature contour distribution in the freeboard.

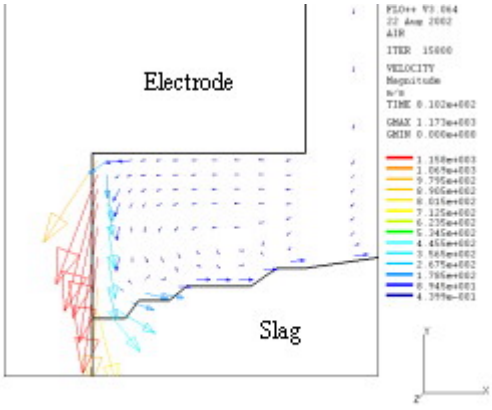

Figure 4. Velocity vector distribution in the arc region.

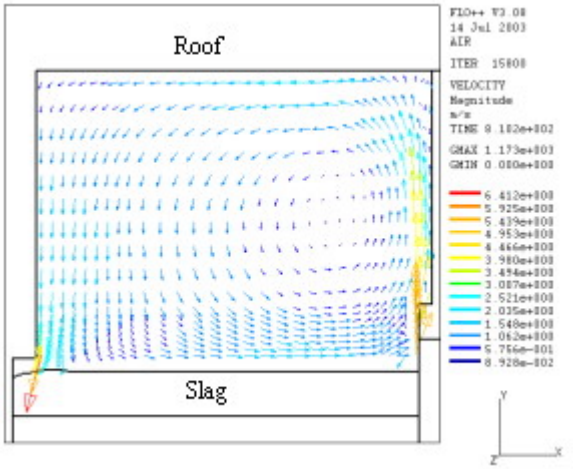

Figure 5. Velocity vector distribution in the freeboard.

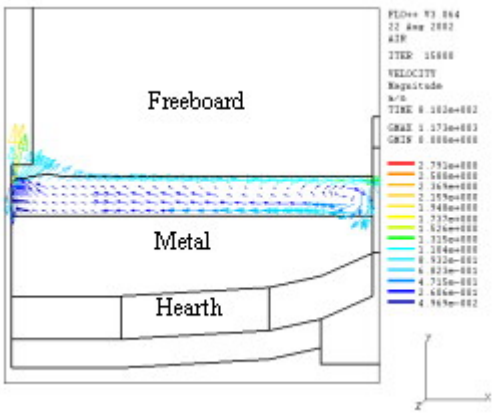

Figure 6. Velocity vector distribution in the slag bath.

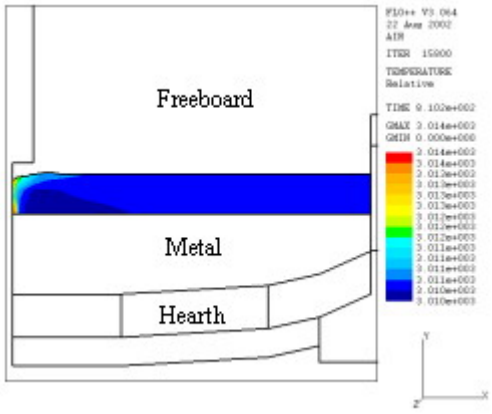

Figure 7. Temperature contour distribution in the slag bath.

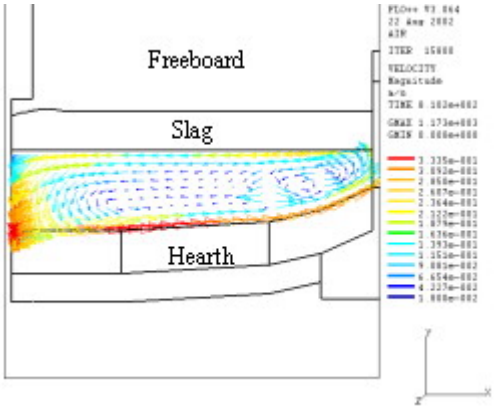

Figure 8. Velocity vector distribution in the metal bath.

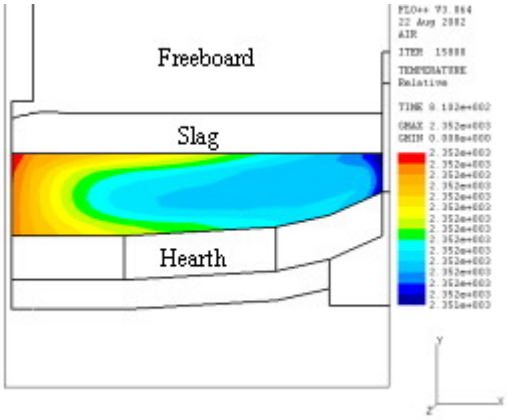

Figure 9. Temperature contour distribution in the metal bath.

The arc induces a clockwise circulation pattern (as viewed) in the slag as a result of the forced convection at the slag-freeboard interface. The slag induces a counter clockwise circulation pattern in the metal as a result of shear coupling across the slag-metal baffle. The buoyancy-driven flow and shear induced flow are mutually reinforcing in the slag. In the metal, the shear- and buoyancy forces oppose, but the shear forces dominate.

The model was repeated with arc lengths of 16, 20, 30, 34 and 38 cm. Figure 10 demonstrates that as the arc length increases, the arc is cooled by additional entrained freeboard gas. The effect of arc length on the arc gas velocity is shown in Figure 11. This demonstrates that the arc velocity increases because the ions in the plasma are accelerated across an increasing potential as the arc length is increased.

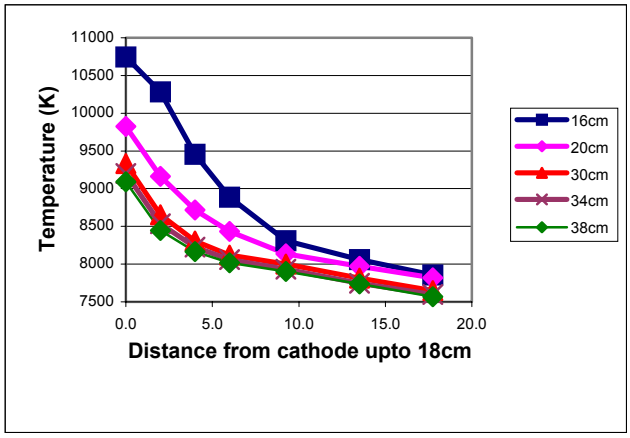

Figure 10. Axial arc temperature vs. axial distance from the cathode at a current of 20kA.

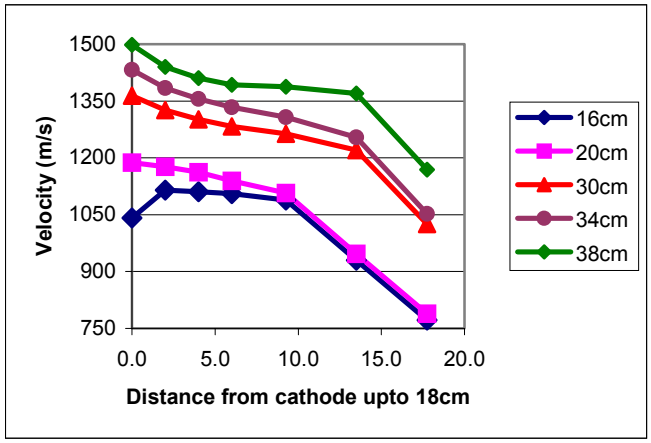

Figure 11. Axial arc velocity vs. axial distance from the cathode at a current of 20 kA.

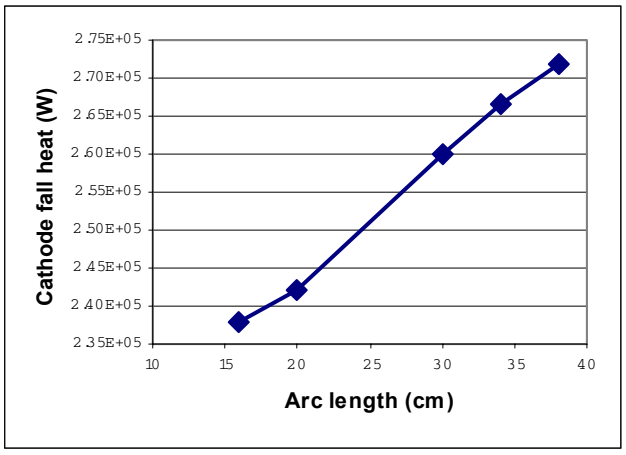

Figure 12. Joule heating vs. different arc lengths at a current of 20kA.

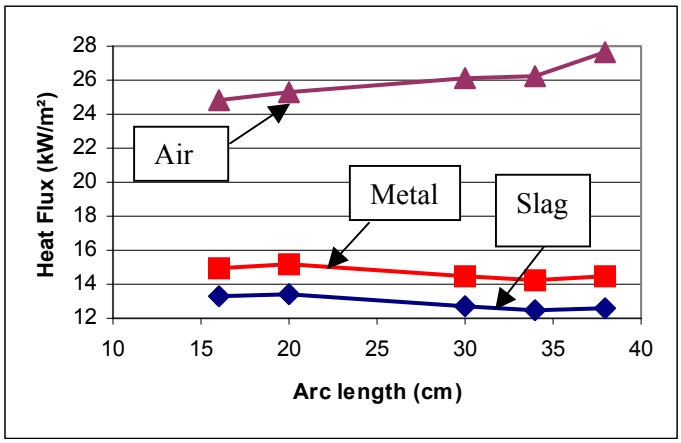

Figure 13. Side wall heat fluxes vs. different arc lengths at a current of 20 kA.

The cathode fall heat[4] in Figure 12 further illustrates that the arc voltage increases as the arc length is increased. Cathode fall energy is as a result of Joule heating in the arc. At constant current, the arc potential increases proportionally with arc length, resulting in an approximately proportional increase in resistive power dissipation.

The dependence of the lower side wall and upper side wall heat flux on the arc length is shown in Figure 13. The heat flux convected to the lower side walls reduces (slightly) with longer arc length, but the additional power in the arc increases the upper side wall heat flux in a similar ratio to the cathode fall heat flow rate. This indicates that lower side wall freeze lining operation can be optimised by adjusting arc length, provided that robust refractory materials are selected for the upper side walls.

5. CONCLUSIONS

The definition and results of a numerical model of an integrated arc furnace were presented. The model was implemented in the Flo++® CFD code and provides for the implicit solution of electrical and magnetic fields, fluid flow and heat transfer through the entire furnace. The results indicate that the model is internally consistent with experimental observation of the response to changes in arc length. The model is capable of assisting with the design of the pyrometallurgical containment vessel geometry, cooling systems and refractory composite, as well as providing valuable information on optimisation of furnace electrical operating parameters.

[4] $Q_C = |J_C|V_C$ [5]

6. FUTURE DEVELOPMENTS

The research completed to date indicated that in order to make the modelling results more comparable to commercial operation, and increase the effectiveness of the design tool, the following features have to be developed:

- Model validation with experimental data.
- Model sensitivity to mesh refining (to optimise processing run time).
- Improved radiation model including provision for radiation absorbtivity of gas cloud especially in the arc (this is currently in progress).
- Full smelting/ melting model to account for process energy and enable different feed positions to be investigated.
- Modelling the effect of chemical reactions in the melt especially CO_2 evolution in the bath as a convective source term.
- Arc depression zone and free surface transient analysis between the freeboard and the slag.
- Dynamic, time dependant arc.

7. REFERENCES

[1] Ushio, M., Szekely, J., and Chang, C.W., "Mathematical modelling of flow field and heat transfer in high-current arc discharge", Ironmaking and Steelmaking, 1981, no. 6, pp. 279-286.

[2] Szekely, J., McKelliget, J. and Choudhary, M., "Heat-transfer fluid flow and bath circulation in electric-arc furnaces and dc plasma furnaces", Ironmaking and Steelmaking, 1983, vol. 10, no.4, pp. 169-179.

[3] Alexis, J., Ramirez, M., Trapaga, G., and Jönsson, P., "Modeling of heat transfer from an electric arc – a simulation of heating – Part I", Electric Furnace Conference Proceedings, 1999, pp. 279-287.

[4] Ramirez, M., Trapaga, G., Alexis, J., and Jönsson, P., "Effects of the Arc, Slag and Bottom bubbling of argon on the fluid flow and heat transfer of a DC EAF Bath – Part II", Electric Furnace Conference Proceedings, 1999, pp. 751-761.

[5] Alexis, J., Ramirez, M., Trapaga, G., and Jönsson, P., "Modeling of a DC Electric Arc Furnace – Heat Transfer from the Arc", ISIJ International 2000, vol. 40, no. 11, pp. 1089-1097.

[6] Ramirez, M., Trapaga, and McKelliget, J., "Fluid flow and heat transfer in steel or steel/slag baths of a DC electric arc furnace under the influence of the arc and gas injection", Paper presented at the Brimacombe Memorial Symposium, 4 October 2000, Vancouver, British Columbia, Canada.

[7] Launder, B. E., and Spalding, D.B., "The numerical computation of turbulent flow", Comp. Meth. in Appl. Mech. & Eng., vol. 3, 1974, pp. 269.

APPENDIX A

Transport Equations

The governing transport and turbulence equations for the arc are expressed in two-dimensional cylindrical coordinates as follow:

Conservation of mass:

$$\frac{\partial(\rho v)}{\partial z}+\frac{1}{r}\frac{\partial(\rho r w)}{\partial r}=0 \tag{1}$$

where: ρ = density, r = radial distance and z = axial distance. The terms v and w are the velocity components in the radial direction and axial direction, respectively.

Conservation of the axial momentum and the axial Lorentz force:

$$\frac{\partial(\rho v^2)}{\partial z}+\frac{1}{r}\frac{\partial(\rho r v w)}{\partial r}=-\frac{\partial P}{\partial z}+2\frac{\partial}{\partial z}\left(\mu_{eff}\left(\frac{\partial v}{\partial z}\right)\right)+\frac{1}{r}\frac{\partial}{\partial r}\left(r\,\mu_{eff}\left(\frac{\partial v}{\partial r}+\frac{\partial w}{\partial z}\right)\right)+J_r B_\theta \tag{2}$$

where: μ_{eff} = effective dynamic viscosity, P = static pressure, J_r = current density in the radial direction and B_θ = magnetic flux density in the azimuthal direction. The product $J_r B_\theta$ is the axial component of the Lorentz force produced by the current and the induced magnetic flux density in the solution domain.

Conservation of the radial momentum and the radial Lorentz force:

$$\frac{\partial(\rho v w)}{\partial z}+\frac{1}{r}\frac{\partial(\rho r w^2)}{\partial r}=-\frac{\partial P}{\partial r}+\frac{\partial}{\partial z}\left(\mu_{eff}\left(\frac{\partial w}{\partial z}+\frac{\partial v}{\partial r}\right)\right)+\frac{2}{r}\frac{\partial}{\partial r}\left(r\,\mu_{eff}\frac{\partial w}{\partial r}\right)-\mu_{eff}\frac{2v}{r^2}-J_z B_\theta \tag{3}$$

where: J_z = current density in the axial direction. The product $J_z B_\theta$ is the radial component of the Lorentz force.

Conservation of thermal energy and the radiation sink term:

$$\frac{\partial(\rho v T)}{\partial z}+\frac{1}{r}\frac{\partial(\rho r v T)}{\partial r}=\frac{\partial}{\partial z}\left(\frac{\mu_{eff}}{\sigma_T}\frac{\partial T}{\partial z}\right)+\frac{1}{r}\frac{\partial}{\partial r}\left(r\frac{\mu_{eff}}{\sigma_T}\frac{\partial T}{\partial r}\right)+\frac{J_z^2+J_r^2}{\sigma_e}-S_R-\frac{5}{2}\frac{k_b}{e}\left(\frac{J_r}{C_p}\frac{\partial T}{\partial r}+\frac{J_z}{C_p}\frac{\partial T}{\partial z}\right) \tag{4}$$

where: T = temperature, C_p = specific heat at constant pressure, σ_T = thermal conductivity, σ_e = electrical conductivity, S_R = radiation sink term, k_b = Bolzmann constant and *e* = electron charge.

Turbulent transport equations

The well-known high Reynolds number k-ε model has been used and will not be discussed in this paper due to space limitations [3], [5], [7].

MHD Approximation

As seen above, the equations for conservation of the axial and radial momentum (2) – (3), include source terms for the Lorentz forces. Thus Maxwell's equations need to be solved.

In flows in which the electric field is of the order of magnitude of the induced quantity **V**×**B,** certain simplifications can be made for Maxwell's equations. This type of flow is usually referred to as MHD (magnetohydrodynamic) flow.

The following assumptions were made for the MHD approximation [5].

- $/V/^2 << c^2$, where c is the speed of light.
- The electric field, E, is in the order of $\mathbf{V}\times\mathbf{B}$.
- The electric energy is negligible compared to the magnetic energy.
- In Ohm's law space energy may be neglected.
- The force density is represented by:

$$f = \rho_e E + J \times B \tag{5}$$

Also, from the Maxwell stress tensor, the electric terms can be shown to be negligible compared to the magnetic terms in this case. For this reason $\rho_c\mathbf{E}$ is taken as negligible in the force density equation [5].

In a two dimensional axis-symmetric system the radial and axial components of the source terms in the momentum equation can be written as:

$$F_r = -J_z B_\theta \tag{6}$$

$$F_z = J_r B_\theta \tag{7}$$

Thus, in order to determine these source terms the current density and the azimuthal magnetic flux density have to be calculated using an MHD approximation. The necessary Maxwell's equation may be written as:

$$\nabla \cdot J = 0 \tag{8}$$

where: **J** is the current density.

Also, for a moving fluid, Ohm's law takes the following form:

$$J = \sigma_e \left[E + V \times B\right] \tag{9}$$

where the first term inside the parenthesis (that is, the electric field, **E**) defines the applied current $\mathbf{J}_{app}$ and the second term defines the induced current $\mathbf{J}_i$.

The electric potential is given by:

$$E = -\nabla\Phi \tag{10}$$

During the development of this model it was assumed that the induced current term could be neglected, that is the magnetic Reynolds number << 1. Thereafter, equations (8), (9) and (10) were combined to obtain the following relationship:

$$\nabla \sigma_e \nabla\Phi = 0 \tag{11}$$

Equation (11) is solved numerically to obtain the electric potential, which is then used to calculate the total current using Ohm's law, equation (9). Thereafter, Ampere's law is employed to approximate the azimuthal magnetic flux density. For an axis-symmetric model this is done as follows:

$$B_\theta = \frac{\mu_p}{r}\int_0^r J_z r dr \tag{12}$$

where: μ_p = magnetic permeability in the media. In these calculations μ_p is assumed to be equal to μ_o.

For further detail regarding the simulation of heat transfer from an electric arc, including the cathode and anode boundary layers, refer to one of the journal papers of Jonas Alexis [3], [5].